

WATER ICE, SILICATE, AND POLYCYCLIC AROMATIC HYDROCARBON EMISSION FEATURES
IN THE *INFRARED SPACE OBSERVATORY* SPECTRUM OF THE CARBON-RICH
PLANETARY NEBULA CPD $-56^{\circ}8032^1$

MARTIN COHEN,² M. J. BARLOW,³ R. J. SYLVESTER,³ X.-W. LIU,³ P. COX,⁴ T. LIM,⁵ B. SCHMITT,⁶ AND A. K. SPECK³

Received 1998 August 18; accepted 1999 January 7; published 1999 January 28

ABSTRACT

Combined *Infrared Space Observatory* Short-Wavelength Spectrometer and Long-Wavelength Spectrometer spectroscopy is presented of the late WC-type planetary nebula nucleus CPD $-56^{\circ}8032$ and its carbon-rich nebula. The extremely broad coverage (2.4–197 μm) enables us to recognize the clear and simultaneous presence of emission features from both oxygen- and carbon-rich circumstellar materials. Removing a smooth continuum highlights bright emission bands characteristic of polycyclic aromatic hydrocarbons in the 3–14 μm region, bands from crystalline silicates longward of 18 μm , and the 43 and 62 μm bands of crystalline water ice. We discuss the probable evolutionary state and history of this unusual object in terms of (a) a recent transition from an O-rich to a C-rich outflow following a helium shell flash or (b) a carbon-rich nebular outflow encountering an O-rich comet cloud.

Subject headings: infrared: ISM: lines and bands — planetary nebulae: individual (CPD $-56^{\circ}8032$)

1. INTRODUCTION

CPD $-56^{\circ}8032$ (hereafter, CPD) belongs to the rare class of late WC-type nuclei of planetary nebulae and is classified as [WC10] in the scheme of Crowther, De Marco, & Barlow (1998). It is thought that such objects may be one result of helium shell flashes in low- and intermediate-mass stars on the asymptotic giant branch (AGB). For a certain fraction of these double-shell-burning stars, a helium shell flash may have ejected or ingested essentially all the remaining hydrogen-rich outer envelope. The resulting star could then be H poor, like the late WC-type ([WCL]) planetary nebula nuclei whose spectra essentially mimic those of bona fide Population I Wolf-Rayet stars, although mostly with lower wind velocities.

The large near- and mid-infrared excess of CPD has been known for over 20 years (Webster & Glass 1974; Cohen & Barlow 1980; Aitken et al. 1980) and has been attributed to emission by dust grains. Mid-infrared emission bands, most often attributed to polycyclic aromatic hydrocarbons (PAHs; e.g., Allamandola, Tielens, & Barker 1989) were detected in ground-based 8–13 μm spectra by Aitken et al. (1980) and in airborne 5–8 μm spectra by Cohen et al. (1989). Longer wavelength PAH bending modes were identified by Cohen, Tielens, & Allamandola (1985) from 7.7–22.7 μm spectroscopy of CPD with the *IRAS* Low-Resolution Spectrometer (LRS). CPD has the highest measured luminosity fraction in the 7.7 μm band of any object (Cohen et al. 1989), and its nebula is characterized by a gas-phase C/O number ratio of 13 (De Marco, Barlow,

& Storey 1997, hereafter DMBS97), which is the joint highest gas-phase C/O ratio measured for a planetary nebula.

We present *Infrared Space Observatory* (*ISO*) Long-Wavelength Spectrometer (LWS; Clegg et al. 1996; Swinward et al. 1996) 43–197 μm full grating spectra of CPD combined with Short-Wavelength Spectrometer (SWS; de Graauw et al. 1996) 2.4–45 μm grating spectra of this object, obtained in the LWS Guaranteed Time program. Preliminary results on the *ISO* spectra of CPD were presented by Barlow (1998).

2. THE *ISO* SPECTRUM OF CPD $-56^{\circ}8032$

Full wavelength coverage grating mode LWS01 spectra of CPD were secured during *ISO* revolution 84. The spectral resolution was 0.6 μm in first order (84–197 μm) and 0.3 μm in second order (43–93 μm). The spectra consisted of eight fast scans, each comprising a 0.5 s integration ramp at each grating position, sampled at 1/4 of a spectral resolution element. Our low-resolution 2.4–45 μm SWS grating spectrum of CPD was taken during *ISO* revolution 273. The SWS01 Astronomical Observing Template was used at speed 1, yielding a mean spectral resolving power of 200–300 over the whole spectrum. Standard pipeline processing (LWS OLP6.0 and SWS OLP6.1) was used to extract, reduce, and calibrate all of the separate spectral fragments. The ISAP and SIA packages provided the capability to examine the spectral fragments in detail.

Figure 1 presents our complete wavelength coverage of CPD, combining SWS and LWS data. First we spliced all of the SWS and LWS subspectra separately, following the methods described by Cohen, Walker, & Witteborn (1992), then joined the composite SWS and LWS portions, which required scaling the LWS spectrum by 0.99 ± 0.01 to register it with the SWS spectrum. The resultant 2.4–197 μm spectrum was normalized to the Point-Source Catalog photometry (see Cohen et al. 1992) in all four *IRAS* bands. This necessitated a further rescaling of the total spectrum of CPD by a factor of 1.05 ± 0.04 .

The *ISO* spectrum of CPD in Figure 1 exhibits unresolved emission lines of [C II] 158 μm , [O I] 63 and 146 μm , and CO rotational lines between $J = 14-13$ at 186.0 μm and $J = 19-18$ at 137.2 μm , which are all excited in the nebular photodissociation region. The canonical spectrum of PAH emission bands dominates the peak of Figure 1 below 15 μm , but the

¹ Based on observations with *ISO*, an ESA project with instruments funded by ESA Member States (especially the PI countries: France, Germany, the Netherlands, and the United Kingdom) with the participation of ISAS and NASA.

² Radio Astronomy Laboratory, 601 Campbell Hall, University of California, Berkeley, Berkeley, CA 94720; mcohen@astro.berkeley.edu.

³ Department of Physics and Astronomy, University College London, Gower Street, London WC1E 6BT, UK.

⁴ Institut d'Astrophysique Spatiale, Bâtiment 121, Université de Paris XI, F-91405 Orsay Cedex, France.

⁵ Space Science Department, Rutherford Appleton Laboratory, Chilton, Didcot, Oxon OX11 0QX, UK.

⁶ Laboratoire de Glaciologie et Géophysique de l'Environnement, CNRS, 54 rue Molière, BP 96, F-38041 Grenoble/Saint Martin d'Hères, France.

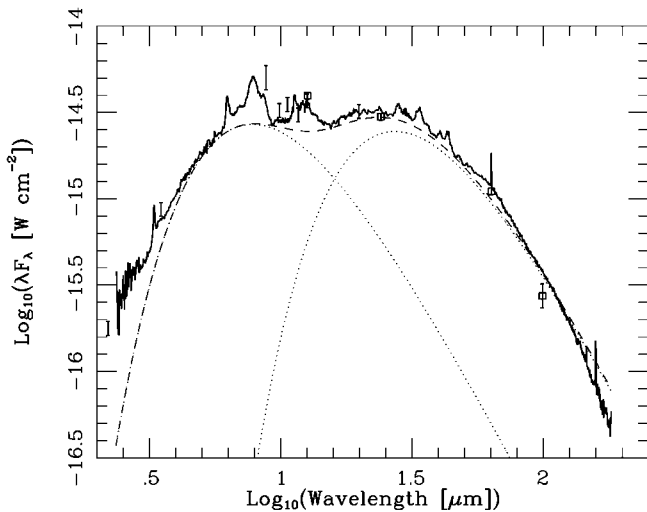


FIG. 1.—Full SWS+LWS spectrum of CPD $-56^{\circ}8032$ (heavy solid line). Also shown are its *IRAS* Point-Source Catalog fluxes (open squares, plotted at their isophotal wavelengths), the 2–20 μm photometry of Cohen & Barlow (1980; bars without points), the continuum we subtracted (short-dashed line), and its two separate blackbody components (dotted line).

most striking aspect is that, despite the carbon-dominated stellar and nebular chemistry, the spectrum longward of 15 μm is dominated by emission features usually associated with the circumstellar envelopes of O-rich stars (Glaccum 1995; Waters et al. 1996; Waelkens et al. 1996). Waters et al. (1998) have presented SWS spectra of two other C-rich planetary nebulae (PNs) with [WCL] nuclei, which also show both PAH and crystalline silicate emission features. The *ISO* spectrum of CPD shown here has an additional remarkable property in that crystalline water ice features are present in emission at 43 and 62 μm (see below).

To identify and quantify the intensities of the many apparent emission bands, we have removed all obvious features from the SWS+LWS spectrum to define a set of continuum points longward of about 4.5 μm . The simplest fit to this continuum was the sum of two blackbodies, with their temperatures and solid angles optimized by least-squares fitting to provide a

lower envelope to the observed spectrum. This lower bound was achieved by ensuring that the difference spectrum (observed minus continuum) is negative only over small wavelength intervals in order to avoid truncating any emission features. The best fit is achieved for temperatures of 470 ± 5 and 135 ± 5 K, which we interpret as grains within the ionized nebula heated by direct starlight (470 K) or by resonantly trapped Ly α photons. Subtraction of this simple continuum yields the CPD “excess” spectrum. Below 5 μm , the steep excess can be attributed to hot grains (~ 1600 K). It is far above the stellar continuum radiation calculated by De Marco & Crowther (1998) and reddened using DBMS97’s value of $E(B-V) = 0.68$, which contributes no more than 5% of the emission at 2.4 μm and rapidly diminishes with increasing wavelength.

The standard PAH emission bands (Cohen et al. 1989) dominate the excess (Fig. 1) with features at 3.3, 5.2, 6.2, 6.9, 7.7, 8.7, and 11.3 μm , together with the underlying emission plateaus at 6–9 and 11–14 μm . Between 16 and 40 μm (Fig. 2, left), several emission features characteristic of crystalline silicates (Glaccum 1995; Waters et al. 1996) are recognizable, most prominently at 19, 24, 28, and 33 μm . The longest wavelength region (Fig. 2, right) exhibits emission bands at 41, 43, 47.5, and 69 μm , along with a very broad, low-level, emission hump centered near 62 μm , under the [O I] 63 μm line. We identify the 43 and 62 μm bands with crystalline water ice, as first detected by Omont et al. (1990) in the Kuiper Airborne Observatory spectrum of the Frosty Leo nebula.

Following Glaccum (1995) and Waters et al. (1996), we have attempted to identify the emission features seen above the continuum of CPD using (a) data for clinopyroxene, orthopyroxene, and 100% forsterite (Koike, Shibai, & Tuchiya 1993) and (b) optical constants for both amorphous and crystalline water ice recently measured in the laboratory (Trotta 1996; Schmitt et al. 1998). We chose the 100% pure forsterite because of its weak but definite feature near 69 μm , shown (according to Koike et al. 1993) only by the pure form of this material. In Figure 2, we distinguish the separate contributions of these four materials and their total. We modeled the optically thin case, for small spherical grains (0.1 or 1.0 μm radius), so that we could neglect scattering and represent Q_{ext} by Q_{abs} . By trying

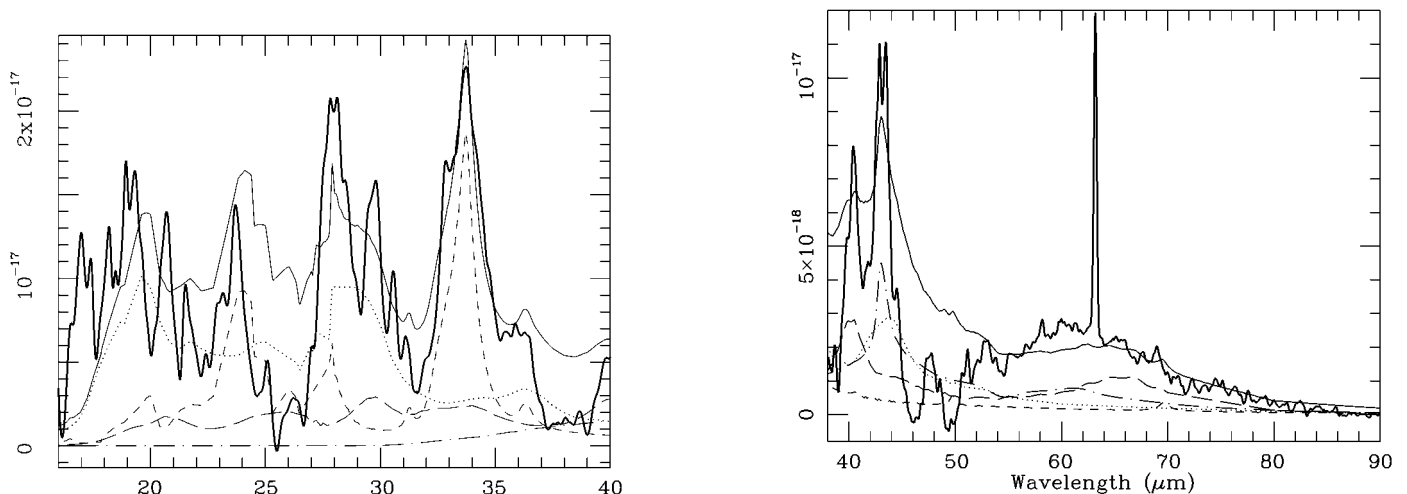


FIG. 2.—Emission from CPD $-56^{\circ}8032$ in excess of the two-blackbody continuum, from 16–40 μm (left) and 38–90 μm (right). In both panels, observed excess emission (heavy solid lines), forsterite (short-dashed lines), clinopyroxene (long-dashed lines), orthopyroxene (dotted lines), crystalline ice (long-dash-dotted lines), and the sum of all these modeled components (light solid lines) are plotted. The units of excess flux are $\text{W cm}^{-2} \mu\text{m}^{-1}$.

to match the relative band strengths, we found plausible temperatures for each component. We made no attempt to constrain these separate temperatures, but three were found to be identical (forsterite, clinopyroxene, and crystalline ice: 65 K) and the orthopyroxene was rather similar (90 K), perhaps suggestive of a common physical location or of core-mantle grains. At these temperatures, the cold silicates produce no measurable emission below the 19 μm band. Note that without combined SWS+LWS coverage, we could not constrain these temperatures.

Our dust modeling indicates that forsterite causes the 24 and 33 μm bands and the weak “wing” at 36 μm . To match the 28 μm band requires crystalline silicates such as orthopyroxene, which also contributes the 19 μm bending mode. Crystalline ice produces features near 43 and 62 μm , due to the transverse optical and longitudinal acoustic vibrational branches, respectively. As noted by Omont et al. (1990), the 62 μm band is not shown by amorphous ice (see the laboratory spectra of Smith et al. 1994), so the observation of this band demands the presence of crystalline ice. The prominent feature near 41 μm is probably dominated by clinopyroxene, and this material also contributes a broad emission feature centered near 66 μm that merges with the longer wavelength ice band.

The sum of our separate component emissions provides only a qualitative match to CPD’s spectrum (Fig. 2), but it is surely indicative of the circumstellar materials present and confirms the striking presence of oxygen-rich materials around a carbon-rich PN. Typically, interband and wing emissions associated with the laboratory features in Figure 2 contribute $\sim 5\%$ of the peak emission. Our lower envelope has not removed such a large continuum, so it appears from Figure 2 that laboratory “crystalline” materials yield features much too broad compared with CPD’s features. Before drawing this conclusion, we would prefer to incorporate these materials into a physically realistic radiative transfer code, including grain geometry and secondary aspects like grain mantle structure and porosity. Note that none of the materials we used to fit the spectrum has a feature matching the one observed at 47.5 μm (Fig. 2, right).

3. DISCUSSION

Using current estimates for the luminosity and distance of CPD, we can deduce the angular extent of each of the emitting dust components around it. Adopting a distance of 1.53 kpc (DMBS97; De Marco & Crowther 1998) implies that if they emit as equilibrium blackbodies, the 470 and 135 K grains we use to represent our dust continuum must lie 36 AU ($0''.02$) and 400 AU ($0''.26$) from the star, respectively. We have derived the distance from the star of the crystalline silicates using optical constants in the UV and visible by Scott & Duley (1996). These materials are transparent in portions of the short-wavelength spectrum but highly absorbing near the UV peak of the energy distribution of the WCL nucleus of this nebula. A realistic energy balance between the UV grain absorption at this peak (we used the non-LTE model atmosphere of De Marco & Crowther 1998) and IR re-emission indicates that the 65–90 K oxygen-rich constituents must lie 1000 AU (0.005 pc) away, i.e., $0''.60$. Thus, even the warmest silicates and ices lie near the periphery of the ionized nebula, based on the *Hubble Space Telescope* images (DMBS97) which show all of the nebular H β emission to be confined to $1''.6 \times 2''.1$. These dimensions, and the normalization factors involved when we fit the emission spectra of grains to the excess emission in CPD, also yield rough estimates of the mass in the crystalline components. We

obtain about 1.6, 1.3, 0.3, and $0.6 \times 10^{-4} M_{\odot}$ for forsterite, clinopyroxene, orthopyroxene, and water ice, respectively, independent of grain size for grain radii less than 3 μm .

Roche, Allen, & Bailey (1986) found the 3.3 μm PAH emission to have an angular size of $1''.3$, i.e., within the ionized boundary of the nebula, while our postulated 470 and 135 K blackbody grains lie well within the carbon-rich nebular ionized gas, suggesting that they too are likely to be carbon-rich (although we cannot prove this). The very hot dust responsible for the excess continuum below 5 μm must be only a few AU from the star and may be condensing in the wind of the WC10 central star, like the dust found to form in the outflows from Population I WC9 stars (e.g., Cohen, Barlow, & Kuhl 1975). Due to the absence of hydrogen in the wind, PAHs cannot be present there; the condensation of hydrogen-deficient soots must occur by pathways that bypass acetylenic chains and emphasize grain formation via fullerenes and “curling” of graphite sheets (e.g., Curl & Smalley 1988). Once such grains later penetrate into the H-rich nebula, partially hydrogenated PAHs may be created. Some nebular PAHs may also have been created previously in a C-rich AGB outflow before it became completely hydrogen depleted.

CPD is not the first PN to have the signatures of both C- and O-rich material recognized. IRAS 07027–7934, found by Menzies & Wolstencroft (1990) to be a low-excitation planetary nebula with a C-rich [WCL] central star (WC10 in the scheme of Crowther et al. 1998), exhibits PAH features in its IRAS LRS spectrum. Yet Zijlstra et al. (1991) discovered that it hosts a strong 1612 MHz OH maser, normally associated only with O-rich material. The Type I bipolar PN NGC 6302 exhibits weak 8.7 and 11.3 μm PAH bands (Roche & Aitken 1986), a weak OH maser (Payne, Phillips, & Terzian 1988), and silicate features at 19 μm (Barlow 1993) and longer wavelengths (Waters et al. 1996). Its LWS spectrum exhibits prominent crystalline water ice emission bands (Barlow 1998; Lim et al. 1999). Waters et al. (1998) have detected crystalline silicate emission features in the SWS spectra of the strongly PAH-emitting C-rich objects BD +30°3639 and He 2-113 (both PNs with cool WC nuclei).

Among hypotheses to explain the simultaneous existence of C- and O-rich particles around C-rich stars, two (Little-Marein 1986; Willems & de Jong 1986) are of possible relevance to CPD and similar nebulae: (a) a recent thermal pulse has converted an O-rich outflow to one that is C-rich; (b) the silicate grains are in orbit around the system and existed well before the current evolutionary phase.

If a recent thermal pulse converted an O-rich mass loss outflow to a C-rich one, the O-rich grains should be farther out and cooler than the C-rich particles, in agreement with the properties of the dust around CPD. The chief objection raised to this scenario, in the context of carbon stars showing warm silicate emission, has been that such a transition should occur only once during the lifetime of a star, so the probability of finding a carbon star with silicate grains in its outflow, still sufficiently close and warm to exhibit a 10 μm feature, should be extremely small. This objection is weakened for extended nebulae, since the cooler nebular particles probe a longer look-back time than do 10 μm emitting silicate grains in a carbon star outflow. The expansion velocity of CPD’s nebula is 30 km s^{-1} (DMBS97), so that nebular material now 1000 AU from the star, the deduced location of the O-rich grains, must have been ejected only 160 yr ago. Even with a lower ($\sim 10 \text{ km s}^{-1}$) typical AGB outflow velocity, the timescale is small compared to the predicted interval of 6×10^4 yr between successive

thermal pulses for a $0.62 M_{\odot}$ core (Boothroyd & Sackmann 1988). Thus a sufficiently recent O-rich to C-rich transition by CPD (as well as by He 2-113 and BD +30°3639) appears statistically improbable, unless, as suggested by Waters et al. (1998), such stars are somehow particularly susceptible to a thermal pulse during their immediate post-AGB phase.

Because of the above difficulty, Lloyd-Evans (1990) and Barnbaum et al. (1991) proposed that carbon stars showing silicate emission are binaries containing a disk in which O-rich grains have accumulated during an earlier evolutionary phase, with the extended disk lifetimes allowing silicate emission to persist. For silicate grains to be warm enough to exhibit a $10 \mu\text{m}$ emission feature, the inner edge of such a disk could be at no more than 4–5 stellar radii from a carbon star (Barnbaum et al.), i.e., 5–6 AU for a $3000 L_{\odot}$, 2400 K star. An O-rich dust disk with these parameters cannot be present around CPD, since it shows no trace of $10 \mu\text{m}$ silicate emission. At a radius of ~ 1000 AU, the cool (65–90 K) O-rich grains would not be in a conventional mass-transfer circumstellar disk around one component of a wide binary, although Fabian & Hansen (1979) have suggested a mechanism whereby a wide binary system might focus matter from one component into a helical trajectory. An alternative possibility that would allow the pre-existing grains hypothesis to be retained would be if they resided in a Kuiper belt or inner Oort comet cloud around the star. A radius of 1000 AU is comparable to current estimates for the outer edge of the Kuiper belt around our own Sun (Weissman 1995)—the interaction of cometary nuclei in such

a belt with CPD's mass outflow and ionization front might provide the conditions needed to liberate the small particles (less than 3–10 μm radius) that are required in order to explain the observed far-infrared silicate and ice bands. The annealing and recrystallization of silicates and ice grains liberated from comets, leading to the required highly ordered structures with correspondingly “sharp” emission features, could result from the sudden increase in the UV photon flux from CPD during its post-AGB evolution. Difficulties for the comet-cloud hypothesis include:

1. The relatively large mass (~ 130 Earth masses) of crystalline silicates derived for CPD, which is high compared to current, although still rather uncertain, estimates for the mass of the solar system Kuiper Belt and Oort Cloud. However, the more massive progenitor stars of current PNs could have appreciably higher mass comet systems.

2. The apparent correlation between the presence of crystalline silicate grains around PNs and the presence of both PAHs and a WCL central star seems to implicate a chemistry change between an O- and C-rich AGB outflow as the cause. However, since this correlation is still based on a small number of objects, the results for a larger sample of nebulae should help clarify whether either hypothesis fits better.

We thank the referee, R. Waters, for his useful comments. M. C. thanks NASA for support under grant NAS5-4884 to University of California, Berkeley.

REFERENCES

- Aitken, D. K., Barlow, M. J., Roche, P. F., & Spenser, P. M. 1980, *MNRAS*, 192, 679
- Allamandola, L. J., Tielens, A. G. G. M., & Barker, J. R. 1989, *ApJS*, 71, 733
- Barlow, M. J. 1993, in *IAU Symp. 155, Planetary Nebulae*, ed. R. Weinberger & A. Acker (Dordrecht: Kluwer), 163
- . 1998, *Ap&SS*, 255, 315
- Barnbaum, C., Morris, M., Likkell, L., & Kastner, J. H. 1991, *A&A*, 251, 79
- Boothroyd, A. I., & Sackmann, I.-J. 1988, *ApJ*, 328, 653
- Clegg, P. E., et al. 1996, *A&A*, 315, L38
- Cohen, M., & Barlow, M. J. 1980, *ApJ*, 238, 585
- Cohen, M., Barlow, M. J., & Kuhl, L. V. 1975, *A&A*, 40, 291
- Cohen, M., Tielens, A. G. G. M., & Allamandola, L. J. 1985, *ApJ*, 299, L93
- Cohen, M., et al. 1989, *ApJ*, 341, 246
- Cohen, M., Walker, R. G., & Witteborn, F. C. 1992, *AJ*, 104, 2030
- Crowther, P. A., De Marco, O., & Barlow, M. J. 1998, *MNRAS*, 296, 367
- Curl, R. F., & Smalley, R. E. 1988, *Science*, 242, 1017
- de Graauw, Th., et al. 1996, *A&A*, 315, L49
- De Marco, O., Barlow, M. J., & Storey, P. J. 1997, *MNRAS*, 292, 86 (DMBS97)
- De Marco, O., & Crowther, P. A. 1998, *MNRAS*, 296, 419
- Fabian, A. C., & Hansen, C. J. 1979, *MNRAS*, 187, 283
- Glaccum, W. 1995, in *ASP Conf. Ser. 73, Millisecond Pulsars—A Decade of Surprise*, ed. A. A. Fruchter, M. Tavani, & D. C. Backer (San Francisco: ASP), 395
- Koike, C., Shibai, H., & Tuchiya, A. 1993, *MNRAS*, 264, 654
- Lim, T., et al. 1999, in preparation
- Little-Marein, I. R. 1986, *ApJ*, 307, L15
- Lloyd-Evans, T. 1990, *MNRAS*, 243, 336
- Menzies, J. W., & Wolstencroft, R. D. 1990, *MNRAS*, 247, 177
- Omont, A., et al. 1990, *ApJ*, 355, L27
- Payne, H. E., Phillips, J. A., & Terzian, Y. 1988, *ApJ*, 326, 368
- Roche, P. F., & Aitken, D. K. 1986, *MNRAS*, 221, 63
- Roche, P. F., Allen, D. A., & Bailey, J. A. 1986, *MNRAS*, 220, 7P
- Schmitt, B., Quirico, E., Trotta, F., & Grundy, W. M. 1998, in *Solar System Ices*, ed. B. Schmitt, C. de Bergh, & M. Festou (Astrophysics and Space Science Library Vol. 227; Dordrecht: Kluwer), 199
- Scott, A., & Duley, W. W. 1996, *ApJS*, 105, 401
- Smith, R. G., Robinson, G., Hyland, A. R., & Carpenter, G. L. 1994, *MNRAS*, 271, 481
- Swinward, B. M., et al. 1996, *A&A*, 315, L43
- Trotta, F. 1996, Ph.D thesis, Univ. of Grenoble, France
- Waelkens, C., et al. 1996, *A&A*, 315, L245
- Waters, L. B. F. M., et al. 1996, *A&A*, 315, L361
- . 1998, *A&A*, 331, L61
- Webster, B. L., & Glass, I. S. 1974, *MNRAS*, 166, 491
- Weissman, P. R. 1995, *ARA&A*, 33, 327
- Willems, F. J., & de Jong, T. 1986, *ApJ*, 309, L39
- Zijlstra, A. A., Gaylard, M. J., te Lintel Hekkert, P., Menzies, J., Nyman, L.-Å., & Schwarz, H. E. 1991, *A&A*, 243, L9